

# Fracture Properties of Ductile Cast Iron used for Thick-Walled Components

**Philip Minnebo**

DG JRC  
Institute for Energy

December 2005



EUR21841EN



### **Mission of the Institute for Energy**

The Institute for Energy provides scientific and technical support for the conception, development, implementation and monitoring of community policies related to energy. Special emphasis is given to the security of energy supply and to sustainable and safe energy production.

### **European Commission**

Directorate-General Joint Research Centre (DG JRC)

<http://www.jrc.cec.eu.int/>

Institute for Energy, Petten (the Netherlands)

<http://ie.jrc.cec.eu.int/>

### **Legal Notice**

Neither the European Commission nor any person acting on behalf of the Commission is responsible for the use, which might be made of this publication. The views expressed in this publication are the sole responsibility of the author and do not necessarily reflect the views of the European Commission.

© European Communities, 2005

Reproduction is authorised provided the source is acknowledged.

*Printed in the Netherlands*

## CONTENTS

1	INTRODUCTION .....	2
2	TEST MATERIAL .....	2
3	EXPERIMENTAL TECHNIQUES .....	3
4	TEST DATA .....	3
5	DISCUSSION .....	4
6	CONCLUSIONS .....	4
7	REFERENCES .....	5
8	TABLES .....	6
9	FIGURES .....	11

## 1 INTRODUCTION

Within the scope of the Joint Research Centre's Action "SAFE-CASK" (EURATOM Framework Programme 6), a comprehensive experimental programme was carried out at the Institute for Energy addressing the inserts of three KBS-3 nuclear waste canisters. Figure 1 shows the overall dimensions of these canisters, which are designed for the deep geological disposal of Boiling Water Reactor spent fuel. The outer shell consists of 50 mm thick copper, providing resistance against corrosion and inside is a thick-walled insert of ductile cast iron to guarantee sufficiently high mechanical strength to withstand the pressure in the deep repository. [1]

A large number of tensile tests were carried out by the Institute for Energy and by the Swedish Foundry Association with specimens from various sampling locations in the three canister inserts. [2] These tensile experiments resulted in significantly varying tensile properties, although the ductile cast iron was always fabricated in accordance with the same standard specification. Low ductility tensile test data could be linked to the presence of specific casting defects, from which so-called "slag" was predominant. [3] A limited series of compression experiments were performed at the Institute for Energy, basically because under deep disposal conditions the largest part of a nuclear waste canister is subject to compressive loading. The compression tests did not result in low-ductility fracture events. [4] Finally the Institute for Energy and the Royal Institute of Technology (Stockholm) jointly performed a programme of fracture tests.

This report presents the results from the fracture toughness experiments completed at the Institute for Energy. The tests were carried out at room temperature and at 0 °C in order to assess the effect of temperature variations under geological disposal conditions. Besides the ductile cast iron material, a number of experimental aspects are discussed. Further, J-integral at fracture initiation and subsequent crack growth resistance are given for various sampling positions within the inserts.

## 2 TEST MATERIAL

The canister insert material investigated is ductile cast iron, which is a cast ferrous material in which the free graphite is in a spherical form. The ductile cast iron is fabricated in accordance with the European standard EN 1563 and corresponds to the grade EN-GJS-400-15U. [5] The standard specifications are primarily based on mechanical properties, which are essentially room temperature tensile data, together with impact and hardness requirements. A typical microstructure is shown in Figure 2. [1] EN 1563 requires a minimum level of nodularity and nodule count.

The canister inserts, which were referred to as I24, I25 and I26, were manufactured by three Swedish foundries as part of the KBS-3 development programme. These thick-walled components were cast in one piece of ductile cast iron. For canister inserts I25 and I26 a bottom pouring casting method was applied whereas insert I24 was produced using a top pouring technique. The chemical analyses corresponding to the three canister inserts are presented in Table 1 although the standard EN1563 does not include any requirement regarding chemical composition.

Fracture specimens were machined from the top and bottom regions of the canister inserts. From the top part both “longitudinal” (parallel to the canister symmetry axis) and “transversal” (perpendicular to this symmetry axis) fracture bars were machined. From the bottom only transversal specimens were fabricated. A typical specimen sampling plan is given in Figure 3. The holes that are apparent from this drawing are present to contain the spent nuclear fuel rods. The actual specimen geometry is shown in Figure 4: it is a standard Single Edge-Notched Bend - SEN(B) - fracture bar with integrated knife edges.

### 3 EXPERIMENTAL TECHNIQUES

ASTM standard E1820 was the basis for performing the fracture toughness experiments, including the fatigue pre-cracking. [6]

Crack growth was always monitored through the elastic compliance method. This crack length measurement technique was calibrated at the start of the pre-cracking process - when the starter notch size was exactly known - by the introduction of an “effective” Young’s Modulus value. At the end of the overall experiment the crack length measurements were adjusted through the optical evaluation of the average fatigue crack length and the average final crack front length.

Pre-cracking was always performed under K controlled conditions. Crack initiation was generally obtained at a  $\Delta K$  value of 18 MPa $\sqrt{m}$ . The intended final fatigue crack length was 18 mm, corresponding to an a/W ratio equal to 0.6. The final  $\Delta K$  was 12 MPa $\sqrt{m}$ . During the entire pre-cracking phase the minimum K level was always 0.1 times the maximum K value.

Following pre-cracking the specimens were side-grooved by two times 1.5 mm. The fracture experiments were carried out on a universal servo-hydraulic test machine under actuator position control, applying a speed of 2 mm/min. Also during the unloading sequences, which reduced the load by 20%, the ramp rate was 2 mm/min. The tests at 0 °C were done in a temperature chamber, using a liquid nitrogen cooling system.

After fracture testing the specimens were cooled down in a liquid nitrogen bath and subsequently opened by means of three-point bending. The fatigue crack and final crack front dimensions were measured by means of a standard stereomicroscope.

### 4 TEST DATA

A considerable number of test specimens showed an irregular final crack front. An obvious example (originating from insert I24) is presented in Figure 5. A lot of these specimens do therefore not meet the ASTM E1820 standard requirement, which states that none of the individual crack size measurements should differ by more than 5% from the average value. Consequently valid  $J_{Ic}$  figures could not be obtained from these test pieces. Nevertheless it was decided to use the results from these experiments and to report the “unqualified”  $J_Q$  values for ALL the tests performed in the scope of this test programme (including the valid experiments!).

Table 2 gives the obtained  $J_Q$  data for all experiments performed at room temperature. Mean values and standard deviations are indicated for the individual sampling positions and for the overall inserts. Table 3 provides the same data obtained from the tests carried out at 0 °C.

Figure 6 shows an example of an R-curve related to insert I25. As is apparent from this figure, the R-curve is in fact defined as a power law fit considering the “qualified” ( $J, \Delta a$ ) data points in between the 0.15 mm and 1.5 mm exclusion lines:

$$J = C_1 \Delta a^{C_2}$$

Tables 4 and 5 present the fitting parameters  $C_1$  and  $C_2$  calculated for the experiments carried out at resp. room temperature and 0 °C. Overall mean values and standard deviations are provided.

## 5 DISCUSSION

First of all it should be stressed that none of the experiments resulted in a brittle (unstable) fracture event. On the other hand it is clear that crack initiation generally took place at relatively low J-integral levels and that the R-curves showed limited crack growth resistance.

From the room temperature experiments it is evident that canister inserts I24 and I25 resulted in comparable J-integral figures near the onset of fracture initiation. Although the data available is limited, it seems that the top longitudinal sampling orientation gives the lowest values for both inserts. For canister insert I26 the global average  $J_Q$  value is significantly lower than observed for I24 and I25. This finding should be related to the higher pearlite content associated with I26. Within the I26 data set the bottom material resulted in the lowest fracture toughness, but this is basically due to one very low test result (12 kJ/m<sup>2</sup>). The standard deviations related to the overall  $J_Q$  measurements are equal for all three inserts. The mean  $C_1$  and  $C_2$  values presented in Table 4 indicate that insert I25 showed the highest crack growth resistance at room temperature. Figure 7 presents three hypothetical R-curves, which are calculated using the average  $C_1$  and  $C_2$  data obtained for the three canister inserts.

It is difficult to draw clear conclusions from the  $J_Q$  data obtained at 0 °C, basically because of the limited amount of test data. Only the I25 and I26 bottom material toughness seems to be affected by this temperature decrease, although the effects are opposite: for I25 lower fracture toughness was measured but with respect to I26 an increasing trend was observed. At 0 °C insert I26 clearly shows the lowest crack growth resistance, as is evident from the power law exponents given in Table 5.

## 6 CONCLUSIONS

- a) No brittle fracture events were observed during the overall experimental programme.
- b) Crack initiation generally took place at relatively low J-integral levels and R-curves showed rather low crack growth resistance.

- c) At room temperature the R-curves measured for canister inserts I24 and I25 were similar. Insert I26, which has a higher pearlite content, showed lower J-values at crack initiation and also the lowest crack growth resistance.
- d) The observations made at room temperature were basically not confirmed by the 0 °C tests.

## 7 REFERENCES

- [1] C.-G. Andersson, P. Eriksson, M. Westman, G. Emilsson, "Status Report Canister Fabrication", TR-04-23, Svensk Kärnbränslehantering AB, June 2004.
- [2] P. Minnebo, "Statistical Analysis of Engineering Tensile Properties of Nuclear Waste Canister Insert Material", EUR21487EN, Joint Research Centre of the European Commission, December 2004.
- [3] P. Minnebo, K.-F. Nilsson, D. Blagoeva, "Tensile, Compression and Fracture Properties of Thick-Walled Ductile Cast Iron Components", Journal of Materials Engineering and Performance, *accepted for publication*.
- [4] P. Minnebo, "Compression Properties of Ductile Cast Iron used for Thick-Walled Components", EUR22101EN, Joint Research Centre of the European Commission, December 2005.
- [5] "Founding - Spheroidal graphite cast irons", EN1563:1997, European Committee for Standardization.
- [6] "Standard Test Method for Measurement of Fracture Toughness", ASTM Standard E1820-01, *Annual Book of ASTM Standards 2002 (Section 3, Volume 03.01)*.

## 8 TABLES

Table 1: chemical analysis (weight percentage) of ductile iron used for producing canister inserts I24, I25 and I26

canister insert	C (%)	Si (%)	Mn (%)	P (%)	S (%)	Cr (%)	Ni (%)	Mo (%)	Cu (%)	Mg (%)
I24	3.66	2.31	0.15	0.03	0.01	0.03	0.27	0.01	0.11	0.05
I25	3.78	2.08	0.21	0.01	0.01	0.04	0.50	---	---	0.04
I26	3.56	2.39	0.52	0.03	0.01	---	0.73	---	---	0.06



Table 2:  $J_Q$  values measured at room temperature for all three canister inserts

	<b>I24</b>	<b>I25</b>	<b>I26</b>
<b>top transversal</b>	44	43	30
		36	33
		30	36
		47	42
-----			
average	44	39	35
standard deviation	--	8	5
-----			
<b>top longitudinal</b>	23	27	37
-----			
<b>bottom transversal</b>	47	48	37
	45	34	26
	39	49	12
	50		
	43		
	37		
-----			
average	45	44	25
standard deviation	5	8	13
-----			
overall average	42	39	32
overall standard deviation	9	9	9
-----			

Table 3: J<sub>Q</sub> values measured at 0 °C for all three canister inserts

	I24	I25	I26
<b>top transversal</b>	--	36	33 34 39
-----			
average	--	36	35
standard deviation	--	--	3
<b>top longitudinal</b>	--	--	--
<b>bottom transversal</b>	47 45 39	30	35 43
-----			
average	44	30	39
standard deviation	4	--	6
overall average	44	33	37
overall standard deviation	4	4	4

Table 4: R-curve fitting parameters  $C_1$  and  $C_2$  for all room temperature experiments

	<b>I24</b>		<b>I25</b>		<b>I26</b>	
	$C_1$	$C_2$	$C_1$	$C_2$	$C_1$	$C_2$
<b>top transversal</b>	69.68	0.34	62.55	0.29	52.80	0.38
			62.97	0.41	51.88	0.31
			52.19	0.40	54.68	0.28
			66.83	0.28	61.84	0.27
<b>top longitudinal</b>	61.66	0.65	59.72	0.57	57.67	0.30
<b>bottom transversal</b>	73.76	0.34	84.36	0.42	56.20	0.28
	73.63	0.28	98.52	0.74	52.02	0.48
	72.82	0.38	99.11	0.51	31.52	0.64
	76.41	0.30				
	78.19	0.43				
	67.04	0.41				
overall average	71.65	0.39	73.28	0.45	52.32	0.37
overall standard deviation	5.35	0.12	18.20	0.15	9.05	0.13

Table 5: R-curve fitting parameters  $C_1$  and  $C_2$  for all 0 °C experiments

	<b>I24</b>		<b>I25</b>		<b>I26</b>	
	$C_1$	$C_2$	$C_1$	$C_2$	$C_1$	$C_2$
<b>top transversal</b>	--	--	71.31	0.47	56.10	0.36
					52.78	0.29
					59.19	0.29
<b>top longitudinal</b>	--	--	--	--	--	--
<b>bottom transversal</b>	73.44	0.31	53.26	0.40	58.60	0.36
	74.02	0.35			61.23	0.25
	72.96	0.44				
overall average	73.47	0.53	62.28	0.43	57.58	0.31
overall standard deviation	0.37	0.06	12.76	0.06	3.25	0.05

## 9 FIGURES



Figure 1:  
overall KBS-3 canister dimensions

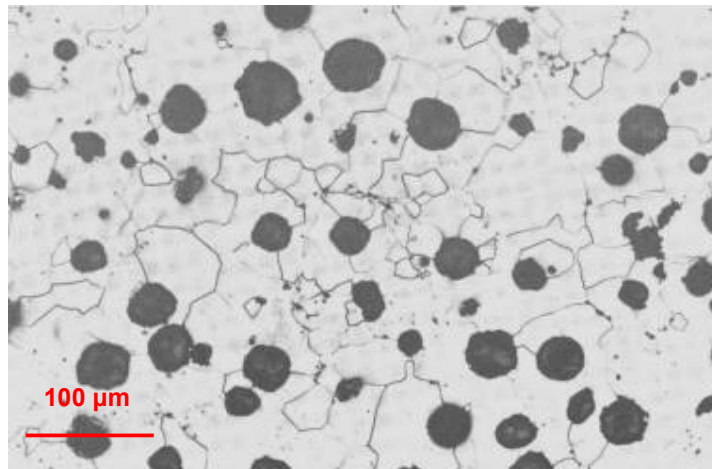


Figure 2:  
typical ductile iron microstructure, showing nodular graphite in ferrite matrix

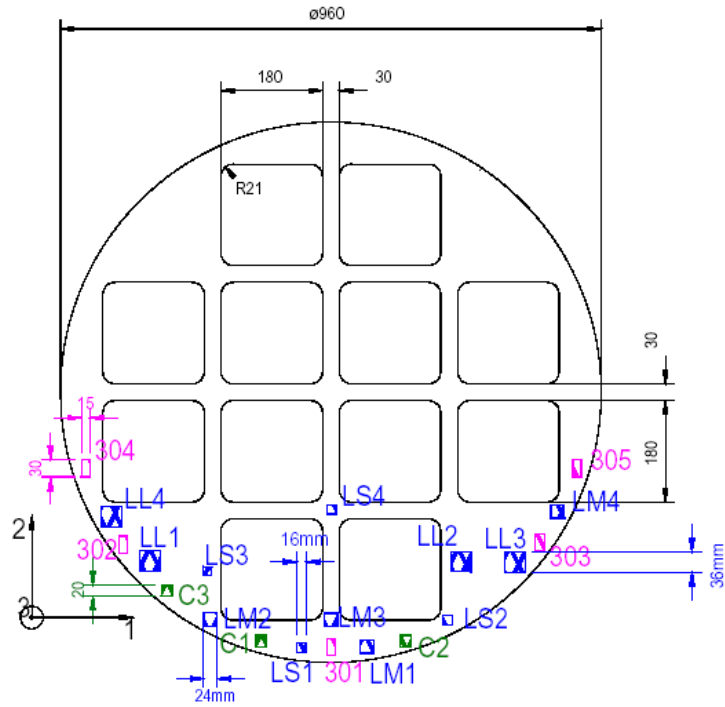


Figure 3:  
example of sampling plan, also showing fracture bars in longitudinal direction  
(code 301 to 305)

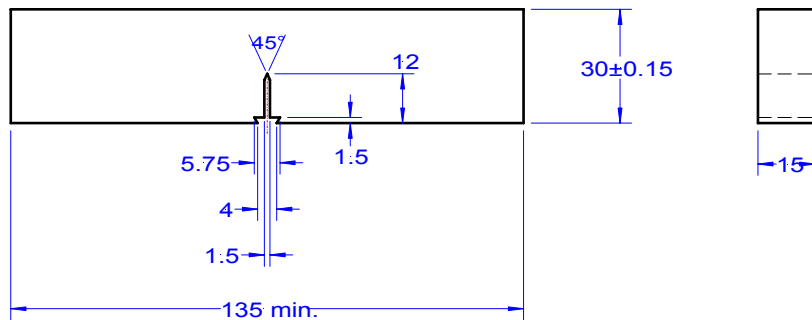


Figure 4:  
fracture specimen design in accordance with ASTM E1820

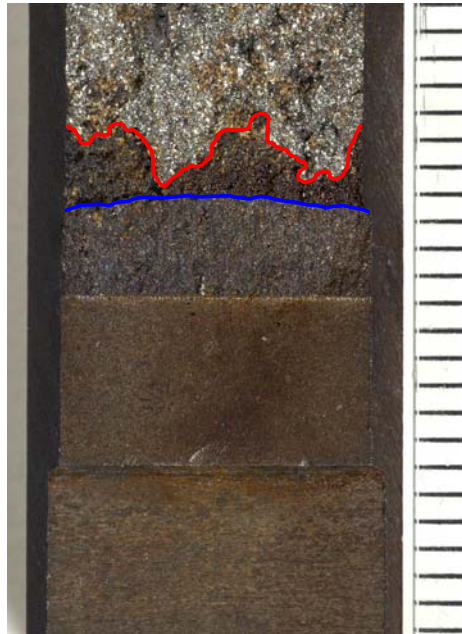


Figure 5:  
fracture surface from insert I24 test specimen, showing irregular final crack front (red)

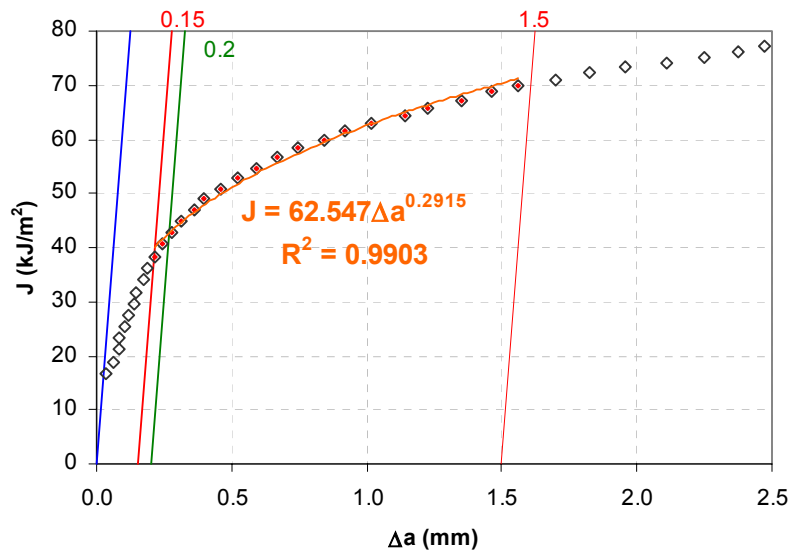


Figure 6:  
R-curve obtained from canister insert I25 material (top transversal specimen)

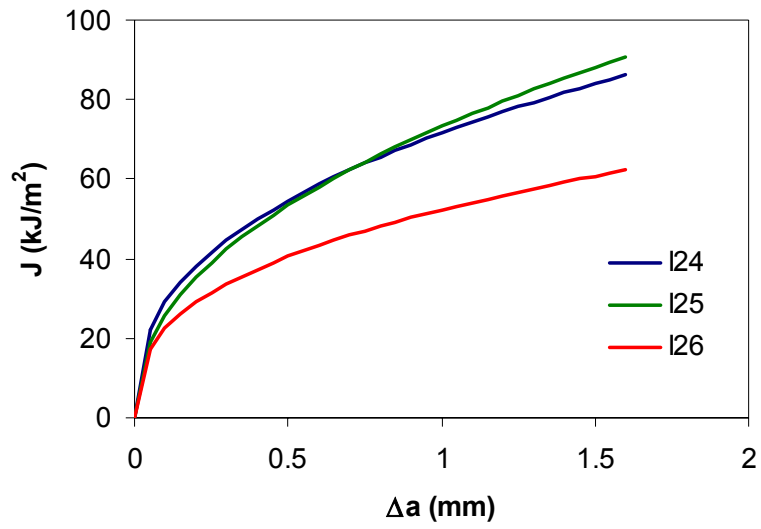


Figure 7:  
hypothetical R-curves, calculated using the average  $C_1$  and  $C_2$  data obtained for  
the three canister inserts (at room temperature)



**European Commission**

**EUR21841EN – DG JRC – Institute for Energy – Fracture Properties of Ductile Cast Iron used for Thick-Walled Components**

**Author: P. Minnebo**

**Abstract**

The report presents the outcome of a programme of fracture experiments addressing three heavy-section components, which were produced from ductile cast iron. No brittle fracture events were observed during the overall test programme. Crack initiation generally took place at relatively low J-integral levels and R-curves showed rather low although stable crack growth resistance.

The mission of the Joint Research Centre is to provide customer-driven scientific and technical support for the conception, development, implementation and monitoring of EU policies. As a service of the European Commission, the JRC functions as a reference centre of science and technology for the Union. Close to the policy-making process, it serves the common interest of the Member States, while being independent of special interests, whether private or national.

